NATURALISTA CAMPANO
ISSN: 1827-7160
Volume 28 Issue 1, 2024

Development of Zno/Cdo Incorporated Activated Carbon Composite for Efficient Phenolic Degradation in Wastewater Treatment

P. S. Abitha[a], S. Grace Victoria[b]

[a]Research Scholar, Department of Physics & Research Centre, Women's Christian College, Nagercoil- 629001, Tamil Nadu, India
Reg.Number: 20113282132011
[b]Assistant Professor, Department of Physics & Research Centre, Women's Christian College, Nagercoil-629001, Tamil Nadu, India
(Affiliated to Manonmaniam Sundaranar University, Abishekapatti, Tirunelveli-627012, TamilNadu, India)
Email: [b]abithafranklin@gmail.com

Abstract: Water contamination has major negative consequences on both human health and environmental sustainability. The use of effective effluent treatment methods is required due to the pollution of water bodies by dangerous substances like phenol and its derivatives. In this study, the effectiveness of a new composite material made of activated carbon (AC) and ZnO/CdO is tested for phenolic degradation. Because of its porous design and high capacity for adsorption, AC makes it easier for organic contaminants to adhere to its catalyst surface, where they may then move to the photoactive ZnO/CdO surface and begin to decompose. XRD, FTIR, SEM and EDAX were used to clarify the structural and chemical characteristics of the synthesised composite material. With an emphasis on the composite's capacity to break down phenolic compounds when exposed to UV or visible light, its photocatalytic activity was assessed using a UV-VIS spectrophotometer. It's significant that the addition of ZnO/CdO to activated carbon for phenolic degradation is a unique strategy for which there are few documented findings. The findings show the promising potential for effective phenol degradation by activated carbon incorporating ZnO/CdO. The composite material has better pollutant removal capacities due to the combination of activated carbon's high adsorption capacity and ZnO/CdO's photoactivity. This study addresses the urgent demand for sustainable freshwater resources by advancing our understanding of the features of the composite and emphasizing its potential for real-world use in wastewater treatment.

Keywords: Wastewater Treatment, Composite Material, ZnO/CdO, Activated Carbon, Phenolic Degradation.

1. Introduction

The majority of the Earth's surface is made up of water, which is a universal material [1]. Additionally, it makes up around 65% of our bodily mass, contributing significantly to our physical make-up. Unpolluted water is valued globally since it is essential for consumption, leisure activities, and aesthetic pleasure [2]. Water contamination, on the other hand, limits its usefulness and has a negative impact on concerns about the economy and beauty. Furthermore, the vast variety of creatures that rely on aquatic environments as well as human health are at danger due to water pollution [3]. A significant ecological concern is the hazard-substance poisoning of rivers and streams. Water pollution is caused by many different things, such as mining activities, sewage discharge, pesticide and fertiliser use, energy production processes, radioactive waste disposal, and urban growth [4]. Particularly large volumes of very hazardous organic waste are produced by the chemical and oil industries. In many industries, phenol and its derivatives are employed as raw materials [5-7]. They have the potential to pollute the environment, particularly water sources.Both natural and human-made mechanisms allow phenol to enter the water [8]. Phenol is naturally produced by the decomposition of dead plants, animals, and organic material in aquatic settings. Phenol is widely used in the chemical and petrochemical sectors for a variety of purposes, demonstrating its adaptability as a crucial ingredient in the synthesis of many chemicals. The importance of phenol in industrial processes highlights the danger to the environment if improperly managed [9]. Additionally, the creation of explosives, textile manufacturing, and dyeing all depend on phenol. It

improves dyeing procedures, aids in the production of synthetic fibres like nylon and polyester, and increases the explosives' stability and potency. These industrial uses highlight how crucial it is to use correct handling, storage, and disposal procedures in order to reduce adverse effects on the environment and public health. Depending on the toxicity level, phenol exposure may have serious negative health impacts on both people and animals. Approximately 9 to 25 mg per kilogramme of body weight have been shown to have harmful effects, and long-term exposure to body weight-dependent dosages may also be harmful [10, 11]. Numerous symptoms, including altered breathing patterns, tremors, muscular spasms, and, in extreme circumstances, respiratory arrest and coma, may be brought on by high exposure levels. Reverse osmosis, coagulation, photo-degradation, chemical oxidation [, membrane filtration, adsorption treatment, chemical precipitation, solvent extraction, ion exchange, nanofiltration, electrochemical techniques, ozonation and biosorption [12-24] are some of the techniques used to address the presence of phenol in water bodies. Every method has benefits and drawbacks, some of which are related to high operating expenses, the production of secondary sludge, increased energy consumption, and the need for significant amounts of chemical reagents. However, photocatalytic pollution degradation has several advantages by drastically lowering disagreeable odours without creating sludge. It is the topic of substantial investigation since it has been shown to be a reliable and safe approach for dye removal. Numerous metal oxide catalysts have been extensively studied and are used in photocatalytic reactions, including TiO_2, CdO, ZnO, Fe2O3, SnO_2, VOx, CuO, CaO, CO_3O_4 and MoOx [25-27]. These catalysts have photocatalytic activity, which makes phenol and its derivatives easier to break down and remove from wastewater. Notably, ZnO and CdO have drawn a lot of interest because of their excellent qualities and wide range of uses[28]. Both ZnO and CdO are regarded as low-cost, non-corrosive, and recyclable materials, making them advantageous for the environment [29]. However, the photocatalytic oxidation process has drawbacks, including ineffective visible light utilisation, difficulties with photoreactor design, limited metal oxide catalyst recovery and reusability, the creation of dangerous intermediates, and worries about environmental impact. Activated carbon (AC) is used as an adsorbent in photocatalytic processes to get over these obstacles and boost their overall effectiveness [30]. Because of its porous structure, large surface area, and moderate adsorption capability, AC is appropriate for applications involving the removal of pollutants. Diverse organic pollutants from wastewater may be effectively removed using the combination of metal oxides and activated carbon. Pollutant adsorption capacity and metal oxide catalyst catalytic efficiency are improved by activated carbon. In this work, we combined activated carbon (AC) with ZnO/CdO using a straightforward method. As a result of the organic pollutants being more easily transferred to the photoactive ZnO/CdO surface due to the surface porosity of AC, the degradation process is accelerated. Utilising methods including Fourier Transform Infrared Spectroscopy (FTIR), X-ray Diffraction (XRD), Scanning Electron Microscopy (SEM), Energy Dispersive X-ray Analysis (EDAX), and UV-VIS spectrophotometry, the synthesised composite material was thoroughly characterised. The chemical and structural properties of the composite material were well explained by these investigations. Using a UV-VIS spectrophotometer, the synthesised composite's photocatalytic activity was assessed. This allowed the evaluation of its capacity to destroy phenolic compounds when exposed to UV or visible light. As there are few published research on the degradation of phenolics utilising activated carbon combined with ZnO/CdO, it is important to note that our study is novel and important. The results of the characterization and evaluation provide insightful information about the characteristics of the composite and its possible use in practical wastewater treatment situations.

2. Material and Methods

2.1. Materials and Chemicals

For the synthesis of photocatalyst Zinc acetate ($C_2H_{15}O_8Zn$ 99%) was purchased from Sigma Aldrich, India and Cadmium acetate ($(CH_3COO)_2$ $Cd.2H_2O$ 99%) was purchased from Sigma Aldrich, India. Sodium hydroxide AR (NaOH, 98%) was obtained from Himedia laboratories, Mumbai were purchased from Qualigens fine chemicals, India. Sigma Aldrich deionized water (H_2O) was used as solvent to prepare solutions with precise concentrations. All the chemicals are used without any additional purification.

2.2 Method of Preparation

Thermal combustion method, commonly known as Auto-Spreading Elevated-Temperature Amalgamation (ASTA), was employed for the preparation of photocatalytic material. This method represents an ingenious and cost-effective approach to produce photocatalyst powders with remarkable purity and uniformity. In this process, an exothermic chemical reaction is initiated between reactants, typically involving metal or metalloid powders and oxidizers, generating an abundance of heat. This internal heat source sustains the reaction and elevates temperatures to levels conducive for synthesizing photocatalytic materials with exceptional

homogeneity and purity. Simultaneously, Solution Combustion Synthesis (SCS) emerges as a remarkably versatile procedure in materials science.

Synthesis of AC ZnO and AC CdO

About 1g of activated carbon is taken in mortar and about 0.5 g of zinc acetate is added to it and grounded for 1 hr. The resulting mixture was transferred into the silica crucible and calcinated at a temperature of 450 °C for 1 hr. The resultant precipitate was noted as ACZnO.

About 1g of activated carbon is taken in mortar and about 0.5 g of Cadmium acetate is added and grounded for 1 hr. The resulting mixture was transferred into the silica crucible and calcinated at a temperature of 450 °C for 1 hr. The resultant precipitate was noted as ACCdO.

Synthesis of AC/ZnO/CdO nanoparticles

In a 250 ml round bottomed flask, 0.5M zinc acetate with 50ml of distilled water and 1M NaOH with 10 ml of distilled water was prepared followed by the addition of 2 grams of activated carbon. The mixture was stirred continuously for two hours. To this (0.2M, 0.4M, 0.6M, and 0.8M) cadmium acetate with 50 ml of distilled water was added in dropwise for 1 hour and stirred. After 1 hour, the solution was filtered using ethanol and water until the precipitate become neutral. Finally the precipitate was washed and dried in hot air oven for 24 hrs at a temperature of 80°C. Then the resultant precipitate was sintered in 450°C for 2 hrs in muffl furnace. The resultant precipitate corresponding to various cadmium acetate concentrations (0.2M, 0.4M, 0.6M and 0.8M) are labelled as AC/ZnO/CdO#1, AC/ZnO/CdO#2, AC/ZnO/CdO#3 and AC/ZnO/CdO#4 respectively that now be used for further investigation and analysis in the chosen topic of study. The preparation of AC/ZnO/CdO photocatalyst is shown in Fig.1

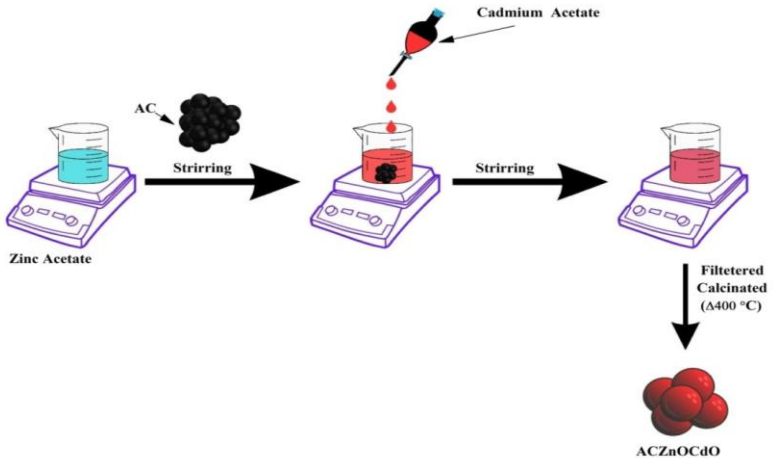

Fig. 1. Preparation of ACZnOCdO photocatalyst.

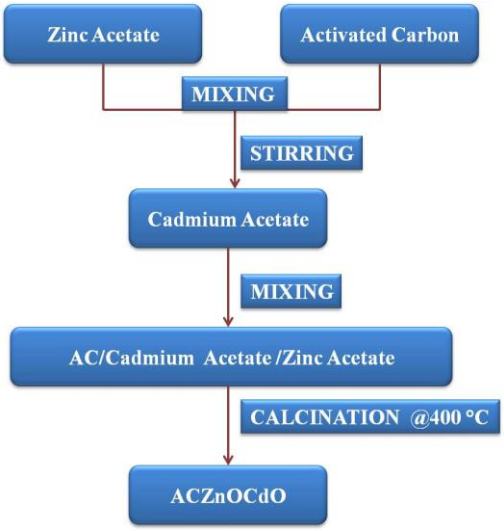

Fig. 2. Schematic representation of ACZnOCdO Photocatalyst synthesis process

2.3 Photocatalytic Degradation Analysis

To initiate the reaction, 50 ml of phenol was poured into a 100 ml beaker. About 2 milligram's of photocatalyst was added to the phenol solution, which was then kept in the dark for two hours to determine the kinetics of adsorption and desorption. The resulting solution was exposed to natural sunlight radiation. Then, aliquots of the solution were removed at every 1 hour intervals, centrifuged, and the rate of variation in phenol concentration during each photocatalytic degradation run was monitored using a spectrophotometer.

To calculate the percentage of pollution degradation, the following formula is used [31]:

% Degradation = $(P_{initial} - P_{final}) / P_{initial} \times 100$

Where:

$\mathbf{P_{initial}}$ = initial absorbance of phenol at a specific wavelength

$\mathbf{P_{final}}$ = absorbance of phenol at the specific wavelength after a certain period of time

The percentage of degradation can be determined by measuring the absorbance of the phenol solution before and after the photocatalytic reaction, and using the formula above. Higher the percentage of degradation, greater the efficiency of the photocatalytic system in degrading phenol.

2.4 Material characterization

The X-ray diffraction analysis of the photocatalyst was performed on an X-ray diffractometer (sample stage 3071/xx) with copper target (λ =1.5405 AU) in theta and 2 theta scan mode. Fourier transform infrared spectroscopy (FTIR) (Thermo Nicolet FTIR spectrophotometer) was employed to investigate the chemical bonding in the powders in the wavelength ranging from 4000 to 400 $cm^{-1.}$ The surface and compositional analysis were examined using SEM/EDAX (JEOL 6390LA/ OXFORD XMX N) instrument for various magnifications. UV-VIS NIR Spectrophotometer is the analytical instrument used to measure the adsorption or transmission of light across a wide range of wavelengths.

3. Result and Discussion

3.1 X-ray Diffraction Analysis

The X-ray diffraction (XRD) analysis of the activated carbon sample revealed a prominent peak in the 22–24° range, confirming the presence of amorphous carbon is shown in Fig.3.

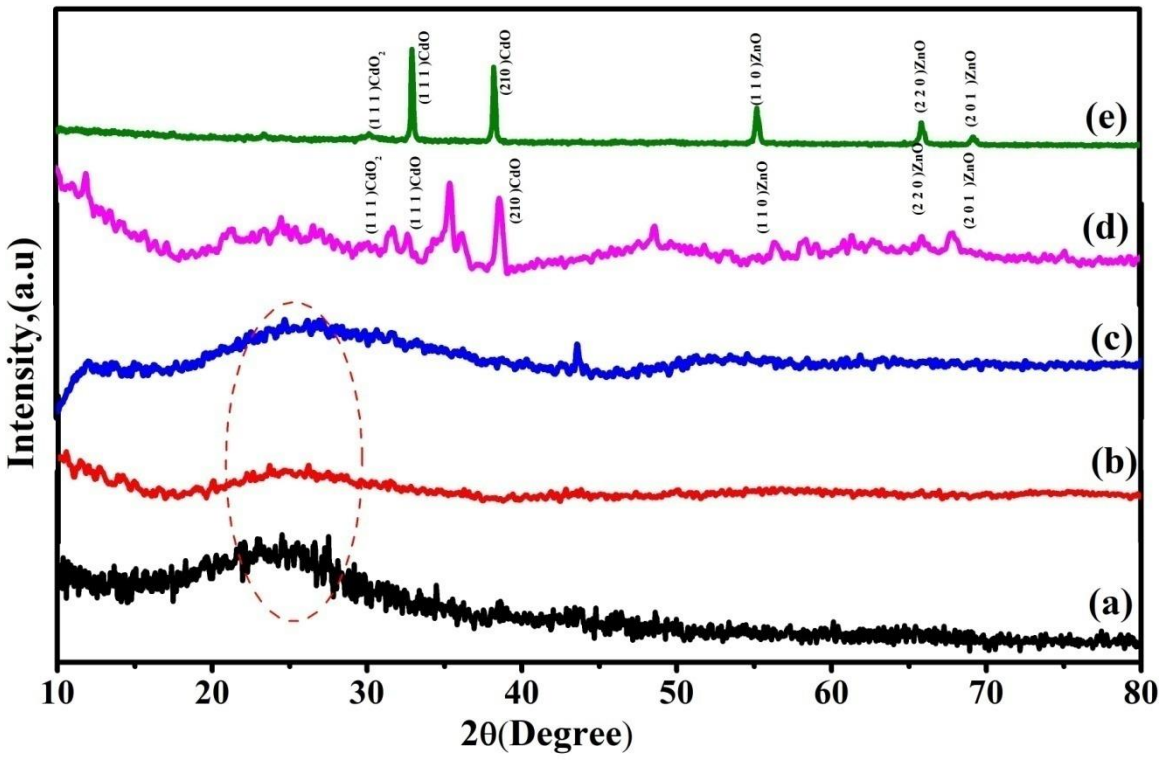

Fig.3. XRD patterns of (a) AC (b) AC/ZnO/CdO#1 (c) AC/ZnO/CdO#2 (d) AC/ZnO/CdO#3 (e) AC/ZnO/CdO#4.

This broad peak signifies a disorganized, long-range arrangement of carbon atoms, contributing to the extensive surface area characteristic of activated carbon. The amorphous structure is advantageous for adsorbing ionic species into its matrix. Additionally, the composite material's XRD analysis identified discrete peaks that corresponded to the zinc oxide (ZnO) (hkl) phases (111), (220) and (201) and that of cadmium oxide (CdO) (hkl) phases (111), (111) and (210). This verification of the presence of significant XRD peaks proves that these elements are present in the composite material. Peaks corresponding to the crystallographic planes of CdO (JCPDS card number 36-1451) 2θ values =30.12,32.46,38.8 [32] and ZnO (JCPDS card number 05-0640) 2θ values = (56.64),(66.04),(67.99) [33] were identified. For Composite (b) AC/ZnO/CdO#1 and (c) AC/ZnO/CdO#2, the XRD spectra displayed a distinctive hum, attributed to the prevalence of the carbon matrix. This suggests a significant role of the amorphous carbon in these composites, as indicated by the broadening of peaks, signifying an amorphous nature that provides a large surface area. This amorphous carbon component serves as an excellent support structure for photocatalysts (ZnO and CdO), facilitating increased surface area interactions and exposure of active sites [34]. The dominance of the carbon matrix in the diffraction pattern emphasizes its contribution to the overall structure of the composite, suggesting potential advantages for photocatalytic applications. On the other hand, the XRD spectra of Composites (d) AC/ZnO/CdO#3 and (e) AC/ZnO/CdO#4 showed clear, strong peaks at 2θ values of (30-31), (32-33), and (38-39), suggesting that CdO is crystalline. Furthermore, peaks at 2θ values of (56-57), (66-67), and (67-68) were detected, indicating that the ZnO is crystalline. These components well-defined crystal lattices suggest that photocatalytic elements have a significant contribution. This crystalline structure is favorable for photocatalysis, providing specific active sites for catalytic reactions, thereby promoting efficient electron transfer and reaction kinetics. In summary, the XRD results suggest that both types of composites hold potential advantages for photocatalytic applications. The amorphous carbon matrix in (b) and (c) enhances surface interactions, while the crystalline nature of ZnO and CdO in (d) and (e) provides specific catalytic sites, collectively contributing to the overall photocatalytic performance of the composites.

Table 1. Position of diffraction peaks (2 θ) of AC/ZnO/CdO photocatalyst

Position of diffraction peaks (2 θ)	**Miller Indices (hkl)**	**JCPDS card no.**
(56.64), (66.04), (67.99)	(110), (220), (201).	36-1451 (ZnO)
(30.12), (32.46) ,(38.8)	((111), (111), (210)	05-0640 (CdO)

3.2 Fourier Transform Infrared Spectroscopy (FTIR) analysis

The FTIR spectrum of modified activated carbon (AC) and AC doped with various metal oxides nanocomposite was analysed in the range of 400–4000 cm^{-1} and is shown in Fig. 4.(a-e).

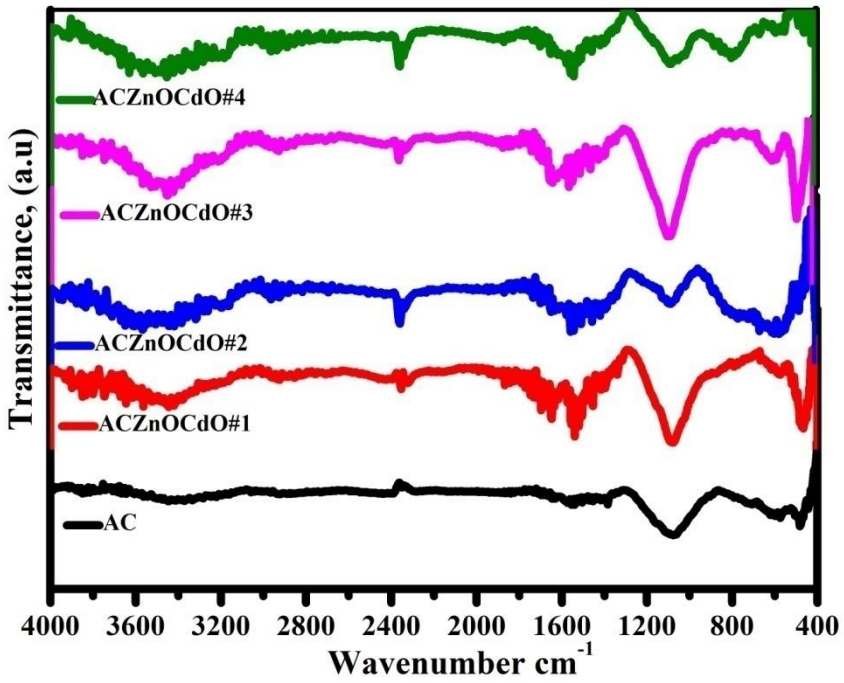

Fig.4. FTIR Spectra of AC (b)AC/ZnO/CdO#1 (c)AC/ZnO/CdO#2 (d)AC/ZnO/CdO#3 (e)AC/ZnO/CdO#4.

In all the broad absorption band observed between 3200 and 3500 cm^{-1} can be attributed to the O-H bond stretching vibration of interlayer water molecules and hydroxyl groups present in the composite matrix. [35]. It denotes the existence of moisture and hydroxyl functional groups connected to the composite's surface. The peak around wavelength of 400-450 cm^{-1} implies the formation of pure ZnO in the composite matrix [36]. As the concentration of CdO increases in the ACZnO matrix, there is an occurrence of peak shift to longer wavelengths indicating the interaction between metal oxide and the AC matrix. This peak shift concordant with the Figure 4(c) (AC/ZnO/CdO#2), the peak is observed at 475 cm-1, while in Figure 4(d) (AC/ZnO/CdO#3) and Figure 4(e) (AC/ZnO/CdO#4), the peak is observed at 510 cm^{-1} and 540 cm^{-1}, respectively. These changes in wavelength indicate the insertion of CdO crystals into ZnO photocatalyst, resulting in altered vibrational characteristics.

3.3 EDAX analysis

The microscopic analysis of the AC/ZnO/CdO composite provides valuable insights into the elemental composition and structural characteristics of the material, as well as highlighting its possible applications in photocatalytic dye degradation. There is a noticeable rise in particle size in the SEM pictures of AC/ZnO/CdO#1, which suggests that ZnO and CdO species are covering the activated carbon matrix more prominently. The observed increase in particle size in AC/ZnO/CdO#2 when compared to the original morphology also implies that the modification in doping concentration has affected particle development, resulting in a more extensive coating of ZnO and CdO species. Analysis of AC/ZnO/CdO#3 reveals an additional rise in particle size. This tendency is consistent with the idea that there is a proportional rise in particle size with increasing ZnO and CdO species doping concentrations.

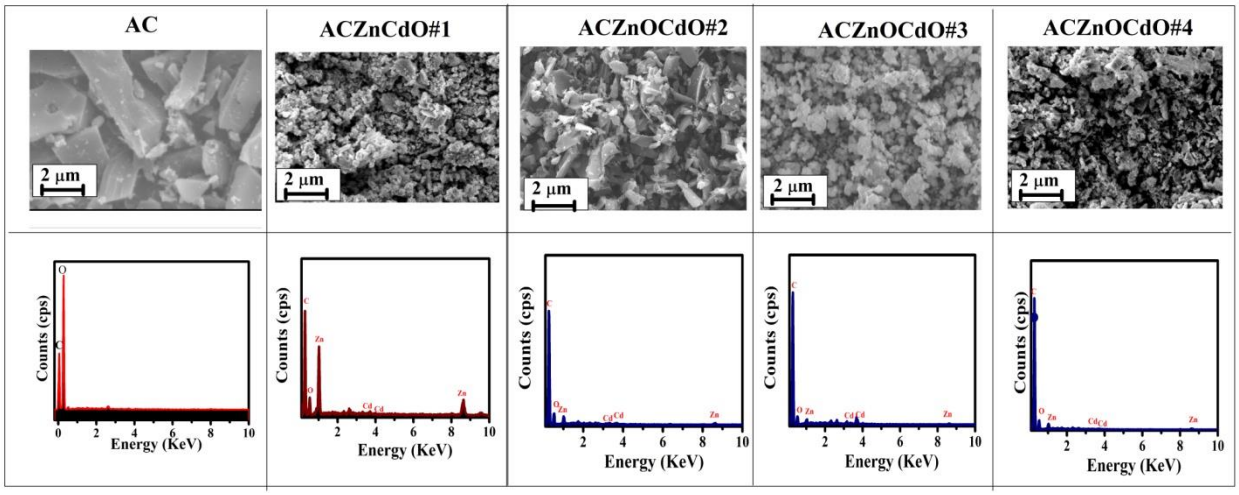

Fig.5. SEM and EDAX image (a)AC (b)AC/ZnO/CdO#1 (c)AC/ZnO/CdO#2 (d)AC/ZnO/CdO#3 (e)AC/ZnO/CdO#4.

Table.2. Elemental composition of AC/ZnO/CdO of various AC/ZnO/CdO photocatalyst

Elements	**AC**	**ACZnOCdO#1**	**ACZnOCdO#2**	**ACZnOCdO#3**	**ACZnOCdO#4**
C	100	84	80.64	85	80
O		11	18.35	14.17	11.87
Cd		1	0.6	0.14	0.73
Zn		4	0.41	0.69	7.4
Total	**100**	**100**	**100**	**100**	**100**

Among the modifications, the SEM pictures of AC/ZnO/CdO#4 show the biggest particle size. This large increase in particle size suggests that ZnO and CdO species are more concentrated, which leads to a thicker coating on the surface of the activated carbon. Notable is also the finding that the shape of particles varies as the doping concentration of ZnO and CdO species varies. Changes in the particle structure are seen in the SEM pictures as the doping concentration changes. More specifically, a rise in concentration causes the quantity of activated carbon flake formations to decrease. On the other hand, a higher concentration causes more needle-like and aggregated morphologies to emerge. The observed change in particle morphology implies that the overall structure of the composite is significantly influenced by the concentration of ZnO and CdO species. The decrease in flake structures and the appearance of needle-like and aggregated morphologies suggest that, at greater concentrations, there is a more thorough coating and interaction between the metal oxide species and the activated carbon matrix. In summary, the analysis of each variation (AC/ZnO/CdO#1, AC/ZnO/CdO#2, AC/ZnO/CdO#3, and AC/ZnO/CdO#4) reveals a consistent trend of increased particle size with higher doping concentrations. This variation in particle morphology is crucial for understanding how changes in composition influence the structural properties of the composite material, providing valuable insights into its potential applications, especially in the context of photocatalytic processes. The EDX analysis further confirms the presence of carbon, oxygen, zinc, and copper as the major elemental constituents in the AC/ZnO/CdO composite. This elemental composition aligns with the expected components based on the synthesis process. The deposition of CdO and ZnO onto the flake-like structure of activated carbon results in the formation of extended and aggregated particles, effectively coating the pores of the activated carbon material. This morphology indicates a strong affinity between the metal oxide photocatalyst and the activated carbon, leading to the formation of a well-integrated composite structure.The addition of activated carbon in the composite plays a vital role in preventing the agglomeration of ZnO and CdO photocatalyst[40]. This interaction between the activated carbon and ZnO-CdO materials leads to the encapsulation of the pore volume of the activated carbon

matrix by the ZnO-CdO species. By encapsulating the pore volume, the composite material effectively restricts electron-hole recombination and minimizes charge carrier loss, which are crucial factors for efficient photocatalytic activity. Moreover, the prominence of the peak corresponding to the cadmium content increases with higher cadmium concentrations. The effective encapsulation of the pore volume, reduced charge carrier loss and increased light harvesting efficiency contribute to the improved performance of the composite material[41, 42]. These findings provide valuable insights into the design and development of advanced photocatalytic materials with enhanced functionality.

3.1. UV DRS Spectrum

The loading amount of CdO within the photocatalyst has a significant influence on their optical absorption characteristics, as evident from the observations presented in Fig. 6a. Notably, the ACCdOZnO#3 photocatalyst exhibit a distinct red shift towards higher wavelengths, accompanied by broad and prominent absorptions within the visible region. This concurrent behavior implies a reduction in the bandgap energy of the ACCdOZnO#3 composite. Conversely, the spectra of the other composites display comparatively lower absorption intensities within the visible range when compared to the AcCdOZnO#3 photocatalyst, indicating a discernible contrast between the two.

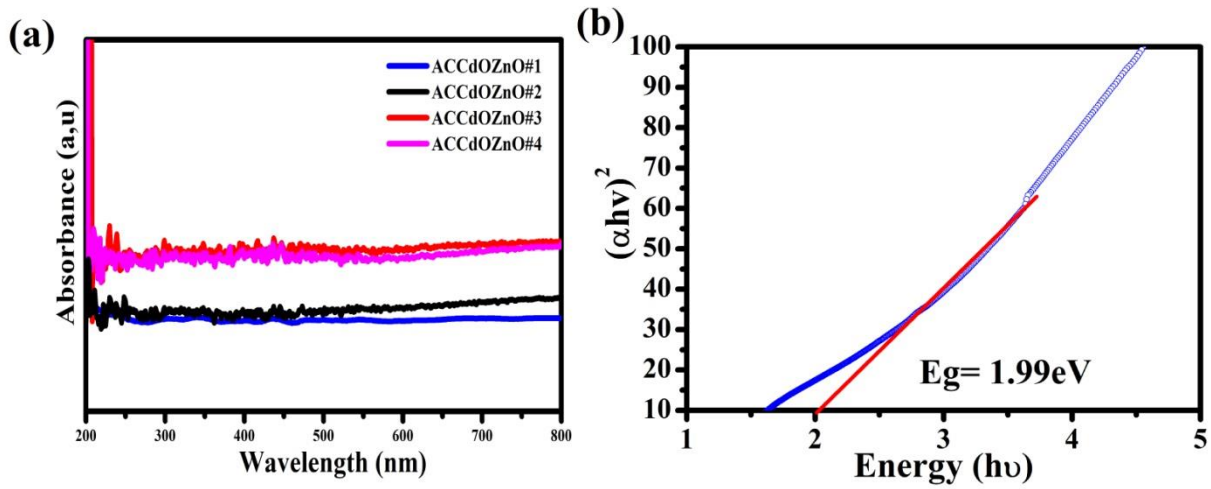

Fig. 6. UV–DRS spectra of various AC/ZnO/CdO photocatalyst and (b) Tauc's plot of ACCdOZnO#3

photocatalyst

To accurately determine the optical bandgap of the photocatalyst, the Tauc's relationship is employed as a reliable method, represented by Equation (2) [43]

$(\alpha h\nu)^n = A(h\nu - Eg)$ ……..(2)

In this equation, the symbols represent the following variables: h denotes the Planck constant, ν represents the frequency of light, α signifies the absorption coefficient of the solid at a specific wavelength, and Eg denotes the bandgap energy. The relationship between these variables is visually illustrated in Figure 7.(b).In this study, the ACCdOZnO#3 photocatalyst was found to possess a bandgap energy of 1.99 eV, which is lower than the values reported in previous literature. This discrepancy suggests that the introduction of CdO and ZnO into the composite material has effectively altered its electronic structure, resulting in a reduced bandgap energy. The lower bandgap energy indicates that the ACCdOZnO#3 photocatalyst is capable of absorbing a broader range of photons with lower energy, thereby extending its absorption into the visible spectrum.The observed decrease in bandgap energy could be attributed to several factors, including changes in the crystalline structure, composition, and doping effects caused by the incorporation of CdO and ZnO. These modifications may introduce additional energy levels within the bandgap, allowing for efficient absorption of visible light and enhancing the photocatalytic performance of the photocatalyst [37].The decrease in bandgap energy observed in the ACCuOZnO#3 photocatalyst can be attributed to the increasing amounts of CdO incorporated into the material. The interaction between CuO and ZnO in these heterostructures plays a crucial role in facilitating charge transfer processes. The presence of CdO and ZnO in close proximity results in an interfacial interaction that promotes the transfer of charges between the two materials. This charge transfer mechanism contributes to

the modification of the electronic structure and, consequently, leads to a reduction in the bandgap energy of the ACCuOZnO#3 photocatalyst. The charge transfer process between CdO and ZnO can occur through various mechanisms, such as electron transfer or the formation of interfacial states. These processes allow for the redistribution of electronic states within the composite material, leading to a change in the energy band structure[44]. As a result, the bandgap energy is effectively lowered, enabling the photocatalyst to absorb photons with lower energy, including those in the visible range.The observed drop in bandgap energy due to the charge transfer between CdO and ZnO highlights the significance of the heterostructure formation and the synergistic effects between the two materials. This phenomenon opens up new possibilities for tailoring the bandgap energies of photocatalyst, offering potential applications in various optoelectronic and photocatalytic devices.

3.2. Photo catalytic studies

The photocatalytic activity of the AC/ZnO/CdO photocatalyst under natural sunlight irradiation was evaluated using a phenol solution, and the results are presented in Figure 7. In the absence of natural sunlight, the AC/ZnO/CdO photocatalyst shows enhanced adsorption properties with the AC at a contact time of 1 hr. This suggests that the addition of CdO and ZnO to the activated carbon influenced the adsorption process, possibly through modifications in the surface charge and acidity of the photocatalysts.

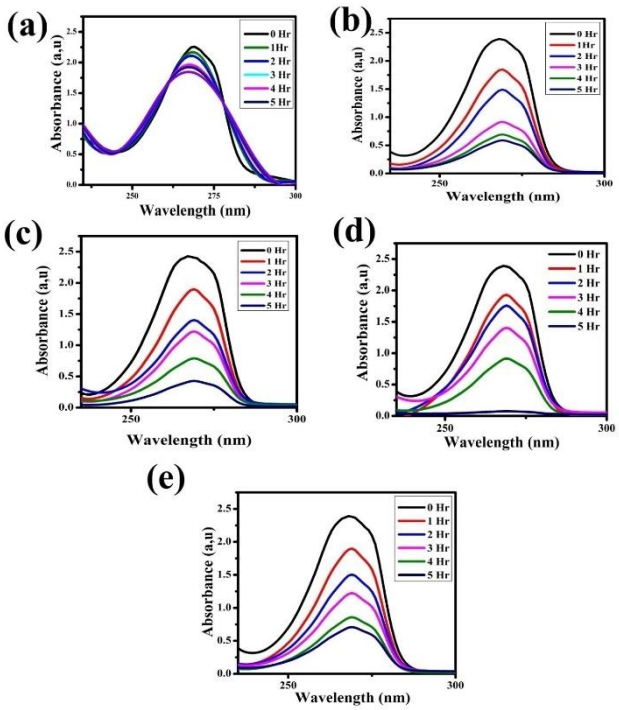

Fig. 7. UV visible adsorption spectra (a) AC (b) AC/ZnO/CdO#1 (c) AC/ZnO/CdO#2 (d) AC/ZnO/CdO#3 (e) AC/ZnO/CdO#4

Under 5 hours natural solar light irradiation, the AC/ZnO/CdO composite demonstrated excellent photocatalytic performance, the photodegradation efficiencies were as follows: AC/ZnO/CdO#1 demonstrated 76%, AC/ZnO/CdO#2 achieved 81%, AC/ZnO/CdO#3 attained 97%, and AC/ZnO/CdO#4 reached 70%. Moreover, it is important to note that 18% of AC's overall efficiency is solely due to the surface adsorption within the AC matrix.The mechanism of photocatalytic degradation of phenol by AC/ZnO/CdO photocatalysts can be divided into three steps. At the initial stage of the reaction the Photocatalyst adsorb the organic pollutants on its surface by the electrostatic attraction between the Photocatalyst and AC matrix. At the second stage the the photodegradation of phenol occurs on the surface of the Photocatalyst by the influence of reactive species. Third, the end products desorb from the photocatalyst surface.

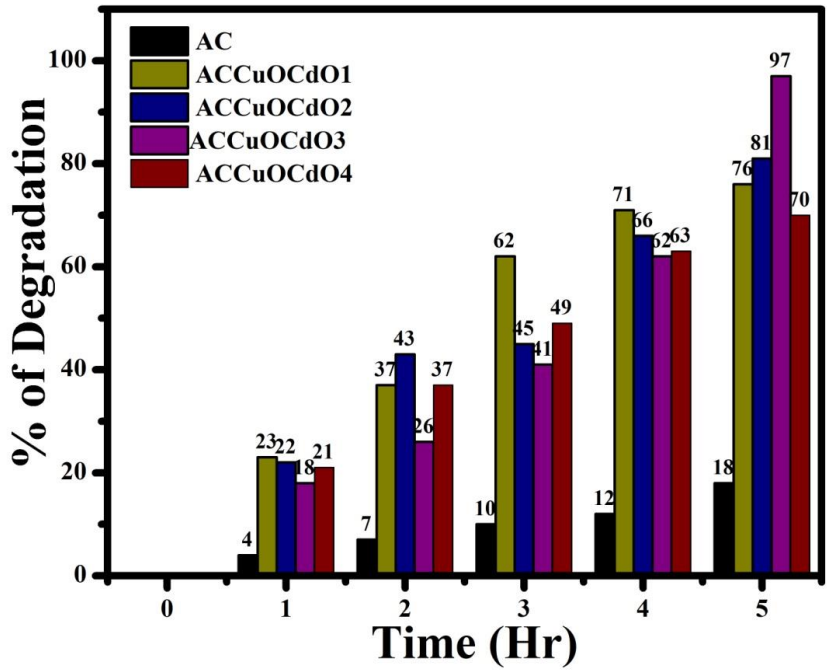

Fig.8. Percentage of Phenol removal AC/ZnO/CdO#1, AC/ZnO/CdO#2, AC/ZnO/CdO#3 and AC/ZnO/CdO#4 against phenol at various time interval.

During solar irradiation, electrons from the valence band (e-) of the semiconductor are excited to the conduction band, creating electron vacancies in the valence band .These electron vacancies (h^+VB) may induce the oxidation of adsorbed phenol molecules on the photocatalyst surface. This process leads to the interaction between the adsorbed water molecules and the generation of hydroxyl radicals (•OH), which subsequently attack the adsorbed phenol molecules. In addition to the generation of hydroxyl radicals, the photochemical formation of superoxide radical ions (O_2•) occurs during irradiation, facilitated by the presence of O_2 in the aqueous solution. The superoxide radicals serve as precursors for various reactive species generated by photochemical reactions. They prevent the recombination of electron-hole pairs in the photocatalyst, thus accelerating the redox reaction. Therefore, photon-generated holes (h+ VB), photo-promoted electrons (e- CB), hydroxyl radicals (•OH), and superoxide ions (O_2•) all contribute to the heterogeneous photocatalytic process under thermodynamically favorable conditions, as depicted in the proposed mechanism and illustrated in the corresponding figure.These photocatalytic processes facilitate the breakdown of organic molecules into intermediates, which can be further degraded into carbon dioxide and water. Overall, the AC/ZnO/CdO composite demonstrates efficient photocatalytic activity under natural sunlight irradiation, showcasing its potential for environmental remediation applications. The understanding of the photocatalytic degradation mechanism provides insights into the underlying processes and guides the development of advanced photocatalytic materials with enhanced performance.

4. Conclusion

The successful synthesis of AC/ZnO/CdO photocatalyst with visible light activity through thermal combustion has been demonstrated. Various characterization techniques, including X-ray diffraction (XRD), Fourier-transform infrared spectroscopy (FTIR), Scanning electron microscopy (SEM) and energy-dispersive X-ray spectroscopy (EDX) confirmed the uniform dispersion of CdO and ZnO on the carbon surface. The AC/ZnO/CdO photocatalyst exhibited significantly enhanced photocatalytic activity compared to unmodified AC and AC CdO photocatalyst. This enhancement was particularly notable in the degradation of phenol under ambient sunlight conditions. The improved photocatalytic performance can be attributed to several factors. Firstly, the presence of CdO and ZnO on the carbon surface provided additional active sites for the adsorption and degradation of phenol molecules. The interaction between the carbon matrix and the CdO-ZnO photocatalyst facilitated efficient charge separation and transfer, minimizing electron-hole recombination and increasing the utilization of solar energy. The visible light activity of AC/ZnO/CdO photocatalyst is of great significance as it expands the range of solar radiation that can be harnessed for photocatalytic applications. This

opens up possibilities for utilizing ambient sunlight, which is more readily available and environmentally friendly, for the degradation of organic pollutants. In conclusion, the synthesis of AC/ZnO/CdO photocatalyst through thermal combustion has been successful, resulting in uniform dispersion of CdO and ZnO on the carbon surface. The enhanced photocatalytic activity of AC/ZnO/CdO photocatalyst, particularly under ambient sunlight, has been demonstrated for the degradation of phenol. These findings contribute to the development of efficient and sustainable photocatalytic materials for environmental remediation applications. Further research and optimization of the AC/ZnO/CdO system could lead to its practical implementation in real-world scenarios for the treatment of water and wastewater contaminated with organic pollutants.

5. References.

1. Chakraborty, S.K. and S.K. Chakraborty, Water: Its properties, distribution, and significance. Riverine Ecology Volume 1: Eco-functionality of the Physical Environment of Rivers, 2021: p. 23-55.
2. Mottl, M.J., et al., Water and astrobiology. Geochemistry, 2007. **67**(4): p. 253-282.
3. Schwarzenbach, R.P., et al., Global water pollution and human health. Annual review of environment and resources, 2010. **35**: p. 109-136.
4. Singh, J., et al., Water pollutants: Origin and status. Sensors in water pollutants monitoring: Role of material, 2020: p. 5-20.
5. Busca, G., et al., Technologies for the removal of phenol from fluid streams: a short review of recent developments. Journal of hazardous materials, 2008. **160**(2-3): p. 265-288.
6. Ali, M.F., E. Ali, and J.G. Speight, Handbook of industrial chemistry. 2005: McGraw-Hill Companies, New York.
7. Mohammadi, S., et al., Phenol removal from industrial wastewaters: a short review. Desalination and Water Treatment, 2015. **53**(8): p. 2215-2234.
8. Khalaf, M.N., Green polymers and environmental pollution control. 2016: CRC Press.
9. Fortuny, A., J. Font, and A. Fabregat, Wet air oxidation of phenol using active carbon as catalyst. Applied Catalysis B: Environmental, 1998. **19**(3-4): p. 165-173.
10. Stamatelatou, K., C. Pakou, and G. Lyberatos, Occurrence, toxicity, and biodegradation of selected emerging priority pollutants in municipal sewage sludge. Comprehensive biotechnology, 2011. **6**(2011): p. 473-484.
11. Villegas, L.G.C., et al., A short review of techniques for phenol removal from wastewater. Current Pollution Reports, 2016. **2**: p. 157-167.
12. Mnif, A., et al., Phenol removal from water by AG reverse osmosis membrane. Environmental Progress & Sustainable Energy, 2015. **34**(4): p. 982-989.
13. Tomaszewska, M., S. Mozia, and A.W. Morawski, Removal of organic matter by coagulation enhanced with adsorption on PAC. Desalination, 2004. **161**(1): p. 79-87.
14. Trillas, M., M. Pujol, and X. Domènech, Phenol photodegradation over titanium dioxide. Journal of Chemical Technology & Biotechnology, 1992. **55**(1): p. 85-90.
15. Yavuz, Y., A. Savas Koparal, and Ü. Bakir Ögütveren, Phenol removal through chemical oxidation using Fenton reagent. Chemical Engineering & Technology: Industrial Chemistry-Plant Equipment-Process Engineering-Biotechnology, 2007. **30**(5): p. 583-586.
16. Raza, W., et al., Removal of phenolic compounds from industrial waste water based on membrane-based technologies. Journal of industrial and engineering chemistry, 2019. **71**: p. 1-18.
17. Djebbar, M., et al., Adsorption of phenol on natural clay. Applied Water Science, 2012. **2**: p. 77-86.
18. Sakurai, A., M. Masuda, and M. Sakakibara, Effect of surfactants on phenol removal by the method of polymerization and precipitation catalysed by Coprinus cinereus peroxidase. Journal of Chemical Technology & Biotechnology: International Research in Process, Environmental & Clean Technology, 2003. **78**(9): p. 952-958.
19. Yang, C., et al., Solvent extraction process development and on-site trial-plant for phenol removal from industrial coal-gasification wastewater. Chemical Engineering Journal, 2006. **117**(2): p. 179-185.
20. Oprea, F. and M. Sandulescu, PHENOL REMOVAL FROM WASTEWATER AND SOUR WATER USING ION EXCHANGE ADSORPTION. Environmental Engineering & Management Journal (EEMJ), 2006. **5**(5).
21. Bódalo, A., et al., Nanofiltration membranes to reduce phenol concentration in wastewater. Desalination, 2009. **245**(1-3): p. 680-686.
22. Abdelwahab, O., N. Amin, and E.Z. El-Ashtoukhy, Electrochemical removal of phenol from oil refinery wastewater. Journal of hazardous materials, 2009. **163**(2-3): p. 711-716.

23. Honarmandrad, Z., N. Javid, and M. Malakootian, Removal efficiency of phenol by ozonation process with calcium peroxide from aqueous solutions. Applied Water Science, 2021. **11**(2): p. 14.
24. Abbas, M.N., et al., Phenol biosorption from polluted aqueous solutions by ulva lactuca alga using batch mode unit. Journal of Ecological Engineering, 2019. **20**(6): p. 225-235.
25. Danish, M.S.S., et al., Photocatalytic applications of metal oxides for sustainable environmental remediation. Metals, 2021. **11**(1): p. 80.
26. Ikram, M., et al., A review of photocatalytic characterization, and environmental cleaning, of metal oxide nanostructured materials. Sustainable Materials and Technologies, 2021. **30**: p. e00343.
27. Gautam, S., et al., Metal oxides and metal organic frameworks for the photocatalytic degradation: A review. Journal of Environmental Chemical Engineering, 2020. **8**(3): p. 103726.
28. Zheng, Z., et al., A fully transparent and flexible ultraviolet–visible photodetector based on controlled electrospun ZnO-CdO heterojunction nanofiber arrays. Advanced Functional Materials, 2015. **25**(37): p. 5885-5894.
29. Weldegebrieal, G.K., H.H. Dube, and A.K. Sibhatu, Photocatalytic activity of CdO/ZnO nanocomposite for methylene blue dye and parameters optimisation using response surface methodology. International Journal of Environmental Analytical Chemistry, 2023. **103**(18): p. 6146-6168.
30. Lim, T.-T., et al., TiO2/AC composites for synergistic adsorption-photocatalysis processes: present challenges and further developments for water treatment and reclamation. Critical Reviews in Environmental Science and Technology, 2011. **41**(13): p. 1173-1230.
31. Sakthivel, S., et al., Solar photocatalytic degradation of azo dye: comparison of photocatalytic efficiency of ZnO and TiO2. Solar energy materials and solar cells, 2003. **77**(1): p. 65-82.
32. Phuruangrat, A., T. Thongtem, and S. Thongtem, Microwave-assisted synthesis of ZnO nanostructure flowers. Materials Letters, 2009. **63**(13-14): p. 1224-1226.
33. Revathi, V. and K. Karthik, Microwave assisted CdO–ZnO–MgO nanocomposite and its photocatalytic and antibacterial studies. Journal of Materials Science: Materials in Electronics, 2018. **29**: p. 18519-18530.
34. Son, E.J., et al., Amorphous carbon nitride as a robust photocatalyst for biocatalytic solar-to-chemical conversion. ACS Sustainable Chemistry & Engineering, 2018. **7**(2): p. 2545-2552.
35. Kasturi, P.R., et al., Preparation of starch-based porous carbon electrode and biopolymer electrolyte for all solid-state electric double layer capacitor. Journal of colloid and interface science, 2019. **554**: p. 142-156.
36. Chen, Y., et al., Structure and photoluminescence of amorphous silicate composites containing ZnO particles synthesized from layered sodium silicate. Journal of non-crystalline solids, 2012. **358**(15): p. 1772-1777.
37. Abbas, S., et al., Characterization of CdO nanoparticles prepared by co-precipitation method under different pH and calcination temperatures. Applied Physics A, 2021. **127**(7): p. 505.
38. Tadjarodi, A. and M. Imani, A novel nanostructure of cadmium oxide synthesized by mechanochemical method. Materials Research Bulletin, 2011. **46**(11): p. 1949-1954.
39. Ravichandran, A., et al., Structural and optical properties of Zn doped CdO nanoparticles synthesized by chemical precipitation method. Journal of Materials Science: Materials in Electronics, 2016. **27**: p. 2693-2700.
40. Sajjad, M., et al., CdO nanocubes decorated on rGO sheets as novel high conductivity positive electrode material for hybrid supercapacitor. Journal of Alloys and Compounds, 2023. **938**: p. 168462.
41. Ibhadon, A.O. and P. Fitzpatrick, Heterogeneous photocatalysis: recent advances and applications. Catalysts, 2013. **3**(1): p. 189-218.
42. Kim, J.H., et al., Hetero-type dual photoanodes for unbiased solar water splitting with extended light harvesting. Nature communications, 2016. **7**(1): p. 13380.
43. Jubu, P.R., et al., Dispensability of the conventional Tauc's plot for accurate bandgap determination from UV–vis optical diffuse reflectance data. Results in Optics, 2022. **9**: p. 100273.
44. Albadarin, N.A., et al., Tunable morphology and band gap alteration of CuO-ZnO nanostructures based photocathode for solar photoelectrochemical cells. Materials Research Express, 2020. **7**(12): p. 125010.
45. Saravanan, R., F. Gracia, and A. Stephen, Basic principles, mechanism, and challenges of photocatalysis. Nanocomposites for visible light-induced photocatalysis, 2017: p. 19-40.
46. Grabowska, E., et al., Metal oxide photocatalysts. 2018.